

In vivo antihyperglycemic effect of *Ptilostemon casabonae* (L.) Greuter leaf extract and its liposomal formulation

Simone Pani^a, Carla Caddeo^{a,*}, Laura Dazzi^a, Giuseppe Talani^b, Enrico Sanna^{a,b}, Arianna Marengo^c, Patrizia Rubiolo^c, Ramon Pons^d, Aurélien Dupont^e, Sonia Floris^a, Cinzia Sanna^f, Francesca Pintus^a

^a Department of Life and Environmental Sciences, University of Cagliari, S.P. Monserrato-Sestu km 0.700, 09042, Monserrato (Cagliari), Italy

^b Institute of Neuroscience, National Research Council (CNR), S.P. Monserrato-Sestu km 0.700, 09042, Monserrato (Cagliari), Italy

^c Department of Drug Science and Technology, University of Turin, via P. Giuria 9, 10125, Turin, Italy

^d Department of Surfactants and Nanobiotechnology, Institute for Advanced Chemistry of Catalonia (IQAC-CSIC), c/Jordi Girona, 18-26, 08034, Barcelona, Spain

^e Biosit – UMS 3480, US S 018, University of Rennes, F-35000, Rennes, France

^f Department of Life and Environmental Sciences, University of Cagliari, via S. Ignazio da Laconi 13, 09123, Cagliari, Italy

ARTICLE INFO

Keywords:

Ptilostemon casabonae extract
Gastro-resistant liposomes
Oral delivery
In vivo assay
Antihyperglycemic effect

ABSTRACT

Prolonged exposure to hyperglycemia is recognized as the primary factor in the pathogenesis of diabetes, a metabolic disease that affects millions of people and one of the top 10 causes of death globally. *Ptilostemon casabonae* (L.) Greuter is an edible plant whose extract has recently shown inhibitory activity against α -glucosidase and antioxidant activity. This suggests that this plant could be a candidate to develop natural remedies against hyperglycemia. In this study, the *in vivo* antihyperglycemic effect of an extract from *P. casabonae* leaves is presented, and a nanoformulation is proposed to possibly enhance such effect, upon oral administration in rats. Liposomes coated with a gastro-resistant polymer, Eudragit, were developed for the loading and delivery of the extract. Nanosized (ca. 90 nm), unilamellar vesicles were produced, as demonstrated by light scattering results and cryo-TEM micrographs. The effects of the loading of the extract and the coating with Eudragit on the liposomes' bilayered structure were described by Small-Angle X-ray Scattering. The physical stability of the *P. casabonae* Eudragit-coated liposomes was evaluated in storage and in simulated gastrointestinal fluids, results showing that the vesicles' key features were preserved. The vesicles efficiently entrapped rutin ($57.4\% \pm 5.7$) and apigenin ($82\% \pm 9.1$), main flavonoids in the extract, as indicated by the quali-quantitative characterization via HPLC-PDA. *P. casabonae* extract was found to exert a significant antihyperglycemic effect in rats subjected to a sucrose load, with a reduction in peak glucose level of 33 and 63 % at doses of 40 and 100 mg/kg, respectively. A 10 mg/kg dose of the extract in Eudragit-coated liposomes produced the same reduction (30 %) as that obtained with a 4-fold higher dose of the extract on its own.

1. Introduction

Hyperglycemia is a growing global health problem that causes diabetes and leads to cardiovascular complications [1–3]. Diabetes is a major metabolic disorder that affects people from almost every country and age group worldwide. In 2021, the number of people with diabetes was estimated to be 537 million, and this number is projected to reach 643 million by 2030 and 783 million by 2045 [4]. Diabetes can affect different organs in the human body and can lead to serious complications, such as cardiovascular diseases and stroke [5]. In addition,

diabetic patients commonly experience neuropathy, nephropathy, retinopathy, kidney diseases and gangrene [6]. Currently, the most common therapies for diabetes include the use of insulin, thiazolidinediones, sulfonylureas and biguanides, which have several side effects.

Plants have traditionally been used, especially in developing countries, to treat various diseases, including diabetes [7,8]. However, only a limited percentage of plant biodiversity has been explored for pharmacological properties [9,10]. Endemic or subendemic species are often understudied due to their restricted range of distribution, despite their phytochemical and biological peculiarities [11]. *Ptilostemon casabonae*

* Corresponding author.

E-mail address: caddeoc@unica.it (C. Caddeo).

<https://doi.org/10.1016/j.jddst.2024.106078>

Received 7 June 2024; Received in revised form 30 July 2024; Accepted 14 August 2024

Available online 22 August 2024

1773-2247/© 2024 The Authors. Published by Elsevier B.V. This is an open access article under the CC BY license (<http://creativecommons.org/licenses/by/4.0/>).

(L.) Greuter is a subendemic plant that grows spontaneously in Sardinia (Italy), Corsica and Hyères Island (France) [12]. Recently, a study examining a hydroalcoholic extract from *P. casabonae* aerial parts revealed the presence of flavonoids (e.g. quercetin and apigenin glycosides) and phenolic acids (e.g. caffeoylquinic acid derivatives) with known antioxidant properties [13]. Furthermore, an extract from *P. casabonae* leaves has shown activity against oxidative stress and α -glucosidase, a target enzyme in diabetes treatment [14]. It is well known that there is a strong correlation between oxidative stress, hyperglycemia and diabetes [15]. Hence, based on this prior knowledge, we hypothesized the use of *P. casabonae* extract against hyperglycemia and on a possible enhancement of its bioactivity by the formulation in nanocarriers, namely liposomes, to be given orally. To this purpose, Eudragit-coated liposomes were used [16]. Eudragit® L100, a poly-anionic copolymer that is insoluble at gastric pH and dissolves above a pH of 6, was used to coat cationic liposomes loaded with *P. casabonae* leaf extract. The gastro-resistant polymer is expected to preserve the liposomes' structure under acidic pH and favor the release of their cargo at near-neutral pH. The features of the Eudragit-coated liposomes key to their functionality were studied, such as size, surface charge, morphology, lamellar structure, entrapment efficiency, and stability in storage and in simulated gastrointestinal fluids. Finally, the anti-hyperglycemic activity of the nanoformulated extract was investigated *in vivo*, in normal rats administered with a sucrose load, and compared with that produced by the extract on its own.

2. Materials and methods

2.1. Materials

Phospholipon 90G (≥ 94 % soy phosphatidylcholine) was purchased from Lipoid GmbH (Ludwigshafen, Germany). Eudragit® L100 was a gift from Evonik Industries AG (Essen, Germany). Stearylamine, phosphate buffered saline (pH 7.4), HPLC-grade acetonitrile (LC-MS grade), formic acid (> 98 % purity), chlorogenic acid, apigenin, rutin and all other reagents, if not otherwise specified, were purchased from Sigma-Aldrich/Merck (Milan, Italy). A Milli-Q purification system (Millipore, Bedford, MA, US) was used to obtain deionized water (18.2 M Ω cm). 1,5-dicaffeoylquinic acid and 1,3 dicaffeoylquinic acid were from Phytolab (Vestenbergsgreuth, Germany).

2.2. Plant material and preparation of *P. casabonae* extract

P. casabonae is not protected by local or international laws, thus its leaves were sampled in Jerzu (Sardinia, Italy) in May 2021, and extracted with 80 % ethanol. The yield of the extract was 11.5 % w/w. The details of the extraction method were previously reported [14].

2.3. Chemical characterization of *P. casabonae* extract

The analysis was performed on a Shimadzu Nexera $\times 2$ system equipped with an SPD-M20A photodiode detector in series to a triple quadrupole Shimadzu LCMS-8040 system with electrospray ionization (ESI) source (Shimadzu, Dusseldorf, Germany), as previously reported [13,14]. Quantification was performed in the UV at the absorption maximum characteristic of the compounds considered: chlorogenic acid ($\lambda = 330$ nm), 1,5-dicaffeoylquinic acid ($\lambda = 330$ nm), rutin ($\lambda = 350$ nm) and apigenin ($\lambda = 340$ nm). Chlorogenic acid, rutin and apigenin were quantified with the calibration curves of their reference standards. 1,3-dicaffeoylquinic acid, 1,5-dicaffeoylquinic acid, succinyl-dicaffeoylquinic acid 1, succinyl-dicaffeoylquinic acid 2, succinyl-dicaffeoylquinic acid 3 and succinylsuccinyl-dicaffeoylquinic acid were quantified at $\lambda = 330$ nm with the calibration curve of 1,5-dicaffeoylquinic acid. Detailed information is given in Table S1.

2.4. Preparation of eudragit-coated liposomes

First, liposomes were prepared by dispersing the phospholipid (P90G) and stearylamine in phosphate buffered saline, with or without *P. casabonae* extract (Table 1), and sonicating for 31 alternate cycles (5 s ON/2 s OFF) + 13 alternate cycles (3 s ON/2 s OFF) using an ultrasonic disintegrator (Soniprep 150 plus, MSE Crowley, London, UK). Second, liposomes were coated by adding dropwise the liposome dispersion to an equal volume of an Eudragit L100 solution (0.1 % w/v in phosphate buffered saline), under gentle stirring [16].

Empty Eudragit-coated liposomes (Table 1) were prepared to evaluate the effect of the extract on the vesicles' features.

Uncoated liposomes, both empty and loaded with the extract (Table 1), were prepared to evaluate the effect of the Eudragit coating and the extract on the vesicles' features.

2.5. Characterization of eudragit-coated liposomes

2.5.1. Average diameter, polydispersity index, and zeta potential

The average diameter, polydispersity index, and zeta potential of the Eudragit-coated liposomes were measured by dynamic and electrophoretic light scattering using a Zetasizer nano-ZS (Malvern Panalytical, Worcestershire, UK). Uncoated liposomes were characterized as well. These three parameters were measured during 90 days to determine the storage stability (at +4 °C) of the vesicles.

2.5.2. Stability in simulated gastrointestinal fluids

The stability of the nanoformulations was evaluated in simulated gastric fluid (0.1 M HCl, pH 1.2) and in simulated intestinal fluid (disodium hydrogen phosphate buffer, pH 7.0; Carlo Erba reagents Srl, Cornaredo, Milan, Italy). 0.3 M Sodium chloride was added to both fluids to increase the ionic strength. *P. casabonae* Eudragit-liposomes were diluted (1:100 v:v) with the simulated gastric or intestinal fluid and incubated for 2 or 6 h (at 37 °C), respectively. The average diameter, polydispersity index, and zeta potential were measured after dilution (t_0) and after incubation (t_2 or t_6). *P. casabonae* uncoated liposomes were analyzed as well.

2.5.3. Entrapment efficiency

The *P. casabonae* Eudragit-coated liposomes were dialyzed against water (for 2 h) to remove the non-incorporated extract components. Both non-dialyzed and dialyzed dispersions were diluted with methanol (1:50 v/v) and analyzed by HPLC-PDA (see Section 2.3). *P. casabonae* uncoated liposomes were analyzed as well. The percentage entrapment efficiency (EE%) was calculated considering quantitative data of characteristic compounds of *P. casabonae* extract (i.e., caffeoylquinic acid derivatives and flavonoids such as rutin and apigenin) in uncoated and Eudragit-coated liposomes using the following equation:

$$EE\% = (\text{compound } \mu\text{g/ml in dialyzed liposomes} / \text{compound } \mu\text{g/ml in non-dialyzed liposomes}) * 100.$$

Table 1

Composition of uncoated and Eudragit-coated liposomes.

	P90G	<i>P. casabonae</i> extract	SA	PBS	0.1% Eudragit
Empty uncoated liposomes	90 mg	–	6 mg	1 ml	
<i>P. casabonae</i> uncoated liposomes	90 mg	4 mg	6 mg	1 ml	
Empty Eudragit-coated liposomes	90 mg	–	6 mg	1 ml	1 ml
<i>P. casabonae</i> Eudragit-coated liposomes	90 mg	4 mg	6 mg	1 ml	1 ml

P90G, phospholipid; *P. casabonae*, *Ptilostemon casabonae* leaf extract; SA, stearylamine; PBS, Phosphate Buffered Saline.

2.5.4. Morphology and lamellar structure

The morphology of the Eudragit-coated liposomes was investigated via cryogenic-Transmission Electron Microscopy (cryo-TEM). Uncoated liposomes were studied as well. The vesicle dispersions (3 μ L) were deposited onto glow-discharged grids, blotted, and vitrified by rapid freezing into ethane. The vitrification process was carried out using an automatic plunge freezer (EM GP, Leica Microsystems Inc., Deerfield, IL, US) under controlled humidity and temperature. The vitrified samples were observed on a 200 kV electron microscope (Tecnai G2 T20 Sphera, FEI Company/ThermoFisher Scientific, Waltham, MA, US) equipped with a 4 \times 4 k CCD camera (TemCam-XF416, TVIPS GmbH, Gilching, Germany). Micrographs were acquired under low electron dose conditions using the camera in binning mode 1 and at a 25,000 \times nominal magnification.

Small-Angle X-ray Scattering (SAXS) analyses were performed to further characterize the liposomes' structure. A description of the equipment and the experimental conditions is reported in De Luca et al. [17]. The SAXS curves were recorded every 20 min for 2 h to check sample stability, then summed up (background was subtracted), fitted using a home-made procedure based on a Gaussian description of the bilayers and a Levenberg-Marquardt minimization scheme [18]. In order to fully represent the available q range, additional structures, in the form of polydispersed spheres, were added. Because of the limited range in which those structures contribute, their parameters (mean particle radius R and polydispersity index PI of the Shultz distribution) cannot be considered fully significant. Because of these limitations, a population of polydispersed cylinders would also provide improved fits. The use of this additional structures was necessary because in the samples that show polydispersity, the Bragg peak appears very close to the upturn of the curves at small q . The error in the parameters was obtained by applying a boot-strapping technique and corresponded to the 95 % confidence interval. The value obtained from the boot strapping was increased if required by systematic error or technique resolution (e.g., for d , the estimated error from the boot-strapping method led to an error of only 0.005 nm, which is below the instrumental resolution at the corresponding q , which is 0.05 nm).

2.6. Animals

Forty-eight male Sprague-Dawley rats (200–250 g) (Charles River, Milan, Italy) were used for the experiments. The animals (four per cage) were housed in polypropylene cages and maintained at a controlled temperature of 22 ± 2 °C and humidity of 50–60 %, with a regular 12-h light/dark cycle. Rats were provided with ad libitum drinking water and standard pellet diet (Stefano Morini, S. Polo D'Enza, Reggio Emilia, Italy). All animal experiments were performed according to the ARRIVE 2.0 guidelines and in compliance with the European Community Council (2010/63/UE L 276 20/10/2010) and the Italian law (DL 04.03.2014, N° 26) for the care and use of laboratory animals. The ethical approval number is 186/2023-PR. Every effort was made to minimize suffering and to reduce the number of animals used.

2.7. Evaluation of antihyperglycemic activity in normal rats

Prior to the experiments, the rats were randomly assigned to control and treatment groups. Each experimental group consisted of eight rats. There were no a priori criteria for inclusion or exclusion of animals.

Rats were fasted overnight, and blood glucose levels were 80.6 ± 1.5 mg/dl ($n = 40$) at the beginning of the experiments. Rats received an intragastric administration (time 0) of different test samples: *P. casabonae* extract dissolved in water containing 1 % Tween 80 was given at the doses of 10, 40 and 100 mg/kg (volume of administration, 3 ml/kg); Eudragit-coated liposomes, which were loaded with *P. casabonae* extract at a concentration of 2 mg/ml, could be tested only at the dose of 10 mg/kg due to the limited volume of intragastric administration; acarbose was given at a dose of 30 mg/kg (volume of

administration, 2 ml/kg) as reference compound and positive control [19]; rats in the negative control groups received an equal volume of vehicle (1 % Tween 80 in water). After 30 min, the rats were loaded orally with a 40 % sucrose solution (dose of 3 g/kg) right after the second blood glucose measurement. Blood glucose was measured again in each rat at 30, 60, 90, and 120 min after sucrose administration. Food, but not water, was withheld from the cages during the experiments. Blood glucose levels were determined by withdrawing a small amount of blood (~ 5 μ L) from the caudal vein and using a standard glucometer (OneTouch Verio Reflect; reported result range: 20–600 mg/dl). Results are expressed as percentage change from basal glucose level and as area under the curve (AUC).

2.8. Statistical analysis

Results are presented as mean values \pm standard deviations (SD). The Student's t -test was performed for pairwise comparisons using Microsoft Excel (Office 365). Differences were considered significant for $p < 0.05$. For the *in vivo* experiments, results are presented as mean \pm standard error (SEM) and represent the percentage change from basal values (glycemia before sucrose administration). For statistical analysis, raw values were used to avoid missing between-group differences. Data were analyzed by two- or one-way ANOVA with treatment (Fig. 4B) and treatment and time (Fig. 4A) as factors, followed by Dunnett's post hoc test with the significance level set at $p < 0.05$, using Prism-GraphPad 10.0 software.

3. Results and discussion

3.1. Characterization of eudragit-coated liposomes and *P. casabonae* extract

This study aimed to develop a vesicle-based formulation, namely liposomes, for the oral delivery of an extract from *P. casabonae* leaves. In order to increase the physical stability of the liposomes and to protect them and their contents from gastric degradation, an enteric polymer (Eudragit) coating was used. *P. casabonae* Eudragit-coated liposomes were prepared and characterized in terms of size, homogeneity and charge and compared with the empty Eudragit-coated and uncoated liposomes to evaluate possible modifications of these parameters induced by the loading of the extract and/or by the coating with Eudragit (Table 2). The empty uncoated liposomes were 78 nm in size and fairly homogeneous (0.28 of polydispersity index) and did not vary upon incorporation of the extract. The surface charge was positive due to stearylamine (Table 2). The coating process led to the formation of larger and more polydispersed vesicles, around 93 nm and 0.37 of polydispersity index, with statistical significance (Table 2). Furthermore, the Eudragit coating significantly affected the surface charge of the vesicles: an inversion of the zeta potential from positive to negative

Table 2

Mean diameter (MD), polydispersity index (PI), and zeta potential (ZP) of *P. casabonae* Eudragit-coated liposomes vs. empty Eudragit-coated liposomes, empty uncoated liposomes, and *P. casabonae* uncoated liposomes. Values are the means \pm SD ($n > 10$). *, ** values statistically different ($p < 0.01$ and $p < 0.001$, respectively) from empty uncoated liposomes; ° values statistically different ($p < 0.001$) from *P. casabonae* uncoated liposomes; § value statistically different ($p < 0.05$) from empty uncoated liposomes.

	MD (nm \pm SD)	PI \pm SD	ZP (mV \pm SD)
Empty uncoated liposomes	78 \pm 5.1	0.28 \pm 0.01	+18 \pm 6.2
<i>P. casabonae</i> uncoated liposomes	78 \pm 3.9	0.28 \pm 0.02	§+15 \pm 5.8
Empty Eudragit-coated liposomes	**92 \pm 5.0	*0.35 \pm 0.04	**−10 \pm 2.8
<i>P. casabonae</i> Eudragit-coated liposomes	°93 \pm 5.4	°0.37 \pm 0.05	°−9 \pm 3.7

values was detected (from +15 to -9 mV; Table 2). This is due to the anionic chains of the polymer that surround the surface of the cationic liposomes.

Fig. 1 shows a representative UV profile of the extract of *P. casabonae*: the identification and the putative identification of the main compounds was based on previously published works [13,14]. Before investigating the entrapment efficiency of the extract in the uncoated and Eudragit-coated liposomes, a comparison was made between the empty liposomes (blank) and those containing *P. casabonae* extract, which excluded the presence of interfering peaks in the blank (Fig. S1).

Some of the most characteristic compounds of the *P. casabonae* extract were quantified to calculate the entrapment efficacy. Seven phenolic acids (caffeoylquinic acid derivatives) and two flavonoids (rutin and apigenin) were selected, as shown in Fig. 1. As for the flavonoids, a different trend was observed for rutin and apigenin: the entrapment efficiency was higher for rutin in the uncoated liposomes ($94.3\% \pm 14.4$ vs. $57.4\% \pm 5.7$ in the Eudragit-coated liposomes; $n = 4$), while no difference was observed for apigenin ($83\% \pm 8.2$ in the uncoated liposomes vs. $82.4\% \pm 9.1$ in the Eudragit-coated liposomes; $n = 4$).

Unexpectedly, for caffeoylquinic acids, the calculated entrapment efficiency gave incoherent values, even above 100% (data not shown). To investigate the behavior of this class of compounds during the encapsulation process, a comparison was made between the profile of the raw extract in solution and that of the extract after the encapsulation process (i.e. non-dialyzed uncoated liposomes). As can be seen in Fig. S2, although the two profiles should be comparable, there are some differences concerning the caffeoylquinic acid derivatives. The amounts of 1,3-dicaffeoylquinic acid (peak 2) and succinylcaffeoylquinic acid (peak 6) increase in the uncoated liposomes, while an opposite behaviour is observed for other compounds, such as chlorogenic acid, 1,5-dicaffeoylquinic acid (peak 4) and succinylcaffeoylquinic acid 1 (peak 5). In particular, the concentration of 1,5-dicaffeoylquinic acid (peak 4) in the raw extract in solution was 62.1 mg/g and decreased to 7.6 mg/g when the extract was incorporated into the uncoated liposomes. At the same time, the concentration of succinylcaffeoylquinic acid 2 (peak 6) increased from 4.1 mg/g in the raw extract in solution to 20.9 mg/g in the uncoated liposomes. In contrast, rutin (peak 3) and apigenin (peak 9) did not show this behavior. For example, the rutin concentration was 17 mg/g in the raw extract in solution and 15.6 mg/g in the uncoated liposomes. This indicates the stability of rutin after the incorporation of the extract into liposomes. These findings confirm the reliability of the results when calculating the entrapment efficiency for flavonoids, in contrast with the incoherent results obtained for the caffeoylquinic derivatives. To better understand the behavior of caffeoylquinic acids after

the encapsulation process, a test with pure 1,5-dicaffeoylquinic acid was performed to monitor possible changes due to the liposomes' preparation process; uncoated liposomes were used as reference (Fig. S3A). The results show that 1,5-dicaffeoylquinic acid underwent some changes during the incorporation into liposomes. In particular, other peaks were detected in the HPLC-PDA profile of 1,5-dicaffeoylquinic acid in both non-dialyzed and dialyzed uncoated liposomes. These peaks are probably due to the conversion of 1,5-dicaffeoylquinic acid into some isomers. The samples were analyzed by HPLC-PDA-MS, which revealed the presence of 1,3-dicaffeoylquinic acid and other dicaffeoylquinic acid isomers at 23.843 min and 26.560 min. The same approach was applied to test the stability of the standard compound rutin after the incorporation into liposomes. As already observed with the whole *P. casabonae* extract, no changes were detected before and after incorporation of rutin into liposomes (Fig. S3B).

Hence, the results obtained with the standard of 1,5-dicaffeoylquinic acid confirmed the unexpected outcomes observed for the caffeoylquinic acid derivatives in *P. casabonae* extract formulated in liposomes. These results are likely due to the described behavior of caffeoylquinic acid derivatives, which may degrade and isomerize under certain conditions. This can be caused for example by cooking processes (e.g. roasting, blanching, baking) and by other conditions, such as temperature, pH, application of ultrasounds. It has been reported that both caffeoylquinic acids and dicaffeoylquinic acids may undergo degradation (e.g. dicaffeoylquinic acid may release monocaffeoylquinic acids) and isomerization (e.g. 3,5-dicaffeoylquinic acid can isomerize to 3,4-dicaffeoylquinic acid and 4,5-dicaffeoylquinic acid), especially under alkaline conditions [20–22].

Compounds identified through the co-injection of an authentic reference standard are marked with a *; the other compounds were putatively identified based on data from Refs. [13,14].

The storage stability of *P. casabonae* Eudragit-coated liposomes was evaluated via monthly measurements of their mean diameter, polydispersity index, and zeta potential. After two months, *P. casabonae* Eudragit-coated liposomes showed a slight increase in size (from 93 to 104 nm) and variations in the polydispersity index (from 0.37 to 0.32) and the zeta potential (from -9 to -6 mV), yet not statistically significant ($p > 0.05$). *P. casabonae* uncoated liposomes displayed a similar trend, with larger size (from 78 to 93 nm; $p > 0.05$) and altered polydispersity index and zeta potential (from 0.28 and +15 mV to 0.34 and +17 mV, respectively; $p > 0.05$). These results point to good medium-term stability of the *P. casabonae* nanoformulation, which was not impacted by the polymer coating.

Since *P. casabonae* Eudragit-coated liposomes were intended for oral administration, their stability in fluids that mimic the gastrointestinal

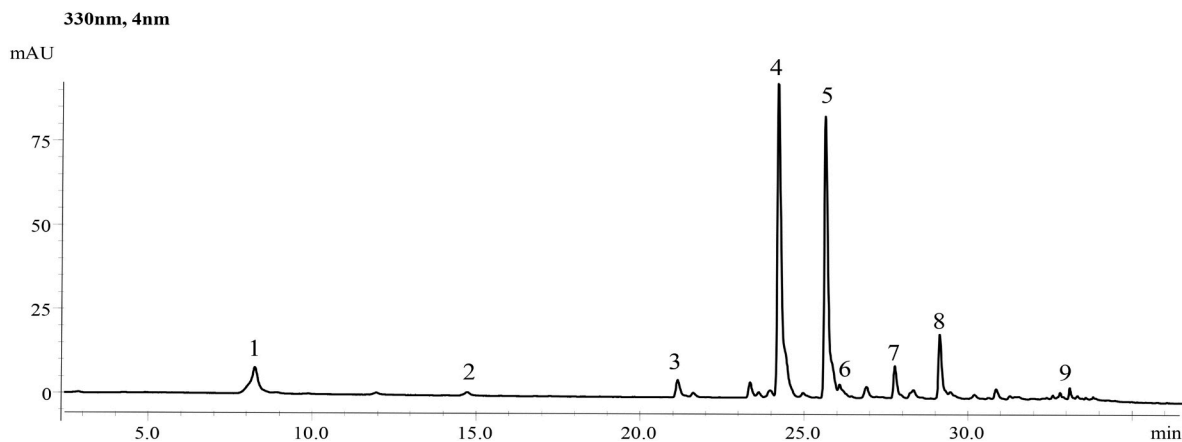


Fig. 1. HPLC-PDA profile of *P. casabonae* leaf extract (2 mg/mL in MeOH 50%) ($\lambda = 330$ nm). Peaks' identity: 1: chlorogenic acid*; 2: 1,3 dicaffeoylquinic acid*; 3: rutin*; 4: 1,5 dicaffeoylquinic acid*; 5: Succinylcaffeoylquinic acid 1; 6: Succinylcaffeoylquinic acid 2; 7: Succinylcaffeoylquinic acid 3; 8: Succinylsuccinyl dicaffeoylquinic acid., 9: apigenin*.

conditions was evaluated and compared to *P. casabonae* uncoated liposomes (Table 3). After 2 h in simulated gastric fluid, *P. casabonae* uncoated liposomes showed an increase in size and polydispersity index (113 nm and 0.41, respectively), with a marked variability within the replicates, while the *P. casabonae* Eudragit-coated liposomes were unaltered, remaining at around 84 nm in size and maintaining a polydispersity index of 0.3. This confirms the effective protection provided by Eudragit against acidic conditions.

The simulated intestinal fluid had a minimal effect on the size and polydispersity of both uncoated and Eudragit-coated liposomes (Table 3). Fluctuations of zeta potential values were detected as a function of the ionic composition of the simulated fluids (Table 3).

The morphological evaluation performed with cryo-TEM indicated that *P. casabonae* Eudragit-coated liposomes (Fig. 2) were characterized predominantly by a unilamellar structure. Some oligolamellar vesicles were also evident. Despite their variable size, which aligns with the polydispersity measured by dynamic light scattering (Table 2), *P. casabonae* Eudragit-coated liposomes presented with regular round shapes and diameters ≤ 100 nm. *P. casabonae* uncoated liposomes demonstrated similar unilamellar structures. Empty Eudragit-coated liposomes presented with less regular shapes in the form of round and elongated vesicles with a higher number of lamellae, similar to empty uncoated liposomes (Fig. 2).

SAXS analyses were performed to deeper characterize the structure of the liposomes.

In Fig. 3A, the experimental scattering curves are presented together with the fits. The shallow maxima around 1.5 nm^{-1} and the secondary maxima around 3.5 nm^{-1} are typical of symmetric phospholipid bilayers. Two different behaviors can be observed: one for the empty liposomes and another for the *P. casabonae* loaded liposomes. The empty liposomes present a faint superimposed maximum around 1 nm^{-1} that can be associated with a certain number of correlated bilayers. This feature is absent in the *P. casabonae* loaded liposomes. A large increase in intensity at small q is noticeable for both empty liposomes and *P. casabonae* loaded liposomes, but larger in magnitude for the former. This can be attributed to the formation of small globular structures that could be tentatively related to the presence of stearylamine and aggregates whose characteristics cannot be determined from SAXS experiments. These globular structures could correspond to very small vesicles. This is in qualitative agreement with the electron microscopy observations showing the presence of small vesicular structures in a larger number for the empty liposomes. Therefore, the calculated

Table 3

Mean diameter (MD), polydispersity index (PI), and zeta potential (ZP) of *P. casabonae* Eudragit-coated vs. uncoated liposomes in simulated gastric fluid (SGF) and simulated intestinal fluid (SIF), measured after dilution (t_0) and after incubation for 2 or 6 h (t_2 or t_6), respectively. Values are the means \pm SD ($n = 4$). *: value statistically different ($p < 0.05$) from *P. casabonae* Eudragit-coated liposomes t_0 .

	Simulated fluid	MD (nm \pm SD)	PI \pm SD	ZP (mV \pm SD)
<i>P. casabonae</i> uncoated liposomes t_0	SGF	85 \pm 4.2	0.28 \pm 0.01	+13 \pm 0.9
<i>P. casabonae</i> uncoated liposomes t_2		113 \pm 35.2	0.41 \pm 0.09	+13 \pm 1.6
<i>P. casabonae</i> Eudragit-coated liposomes t_0	SGF	82 \pm 3.0	0.28 \pm 0.04	+11 \pm 1.7
<i>P. casabonae</i> Eudragit-coated liposomes t_2		84 \pm 4.1	0.30 \pm 0.04	+11 \pm 1.2
<i>P. casabonae</i> uncoated liposomes t_0	SIF	87 \pm 5.5	0.32 \pm 0.05	-1 \pm 0.7
<i>P. casabonae</i> uncoated liposomes t_6		88 \pm 1.0	0.37 \pm 0.04	-1 \pm 2.3
<i>P. casabonae</i> Eudragit-coated liposomes t_0	SIF	84 \pm 7.5	0.31 \pm 0.03	-1 \pm 0.7
<i>P. casabonae</i> Eudragit-coated liposomes t_6		87 \pm 3.2	*0.38 \pm 0.02	-2 \pm 0.6

polydispersity index PI of the Shultz distribution and mean particle radius R (Table 4) are only indicative of the order of magnitude.

The fits of the model used were quite good, as can be appreciated graphically in Fig. 3A and from the reduced chi squared χ^2 values close to 1 (Table 4). The values obtained for the multilayers (N_c ; Table 4) and the repetition distance (d ; Table 4) are similar to those found for liposomes previously prepared with the same phospholipid [23]. The amount and correlation of the multilayers are limited to few multilayers with a low interlayer correlation (high η_1 values; Table 4). Concerning the rest of the parameters, the values are similar for the empty and *P. casabonae* loaded liposomes. The main differences are the larger bilayer hydrophobic thickness (Z_H ; Table 4) and the methyl Gaussian amplitude (σ_G ; Table 4) for the *P. casabonae* loaded liposomes, which are congruent with the solubilization of hydrophobic molecules such as fatty acids present in *P. casabonae* extract [14]. Statistically significant differences are also found in the headgroup amplitude (σ_H ; Table 4), but it is difficult to understand those changes due to the complexity of the extract. The higher polar head density (ρ_H ; Table 4) could be due to the preferential adsorption of some electron-rich molecules of the extract onto the polar headgroups.

Overall, the results point to a major effect on the liposomes' bilayer structure induced by the incorporation of the *P. casabonae* extract rather than the coating of the polymer.

3.2. Antihyperglycemic activity of *P. casabonae* extract in normal rats

The basal blood glucose, measured after an overnight fast (time 0), was $80.6 \pm 1.5 \text{ mg/dl}$ ($n = 48$). The intragastric administration of sucrose (3 g/kg) increased the blood glucose to a peak of $104.1 \pm 18.2 \%$ with respect to basal value, at 30 min. In subsequent measurements taken at 30-min intervals, the blood glucose decreased slowly and had not returned to basal levels ($+78 \pm 12.7 \%$) 120 min after sucrose administration (Fig. 4A).

The antihyperglycemic effects of intragastric administration of increasing (10, 40 and 100 mg/kg) doses of *P. casabonae* extract dissolved in water are shown in Fig. 4. The glycemic curves showed a clear dose-dependent glucose peak reduction (Fig. 4A), and a significant difference ($p < 0.001$) was detected between the 40 and 100 mg/kg doses, with peak values of $70.2 \pm 11.1 \%$ and $38.5 \pm 17.1 \%$, respectively, compared to the negative control. These effects on the sucrose-induced hyperglycemic peak were paralleled by a significant reduction in the AUC, as shown in Fig. 4B. The intragastric administration of acarbose – an antidiabetic reference compound (30 mg/kg, p.o.) – significantly ($p < 0.01$) reduced both the blood glucose peak ($23.0 \pm 16.6 \%$ at 30 min vs. basal values, Fig. 4A) and the AUC by 73 % (Fig. 4B) compared to the negative control (vehicle + sucrose).

Animal models, particularly mouse and rat, are often used to test antidiabetic agents, including plant compounds [24]. These models are essential for validating the *in vitro* inhibition of carbohydrate hydrolyzing enzymes, such α -glucosidases and α -amylase, responsible for the increase of postprandial blood glucose levels. The present *in vivo* results support our previous *in vitro* findings suggesting the antihyperglycemic potential of the *P. casabonae* extract based on the effective inhibition of α -glucosidase [14]. The data obtained in this study, although relatively limited in the range of tested concentrations, show that doses as low as 40 mg/kg of the aqueous solution of the extract produced an effective antihyperglycemic effect in normal rats loaded with sucrose, and also show that the maximum dose tested (100 mg/kg) produced an antihyperglycemic effect comparable to that elicited by antidiabetic acarbose at a dose of 30 mg/kg. These data suggest that it may be highly valuable to pursue further research to identify the component/components of the extract that are responsible for this pharmacological activity.

Sanna et al. [14] reported the absence of cytotoxicity in Caco-2 cell line at the extract concentration required to inhibit α -glucosidase almost completely, which may suggest an adequate safety profile. In partial

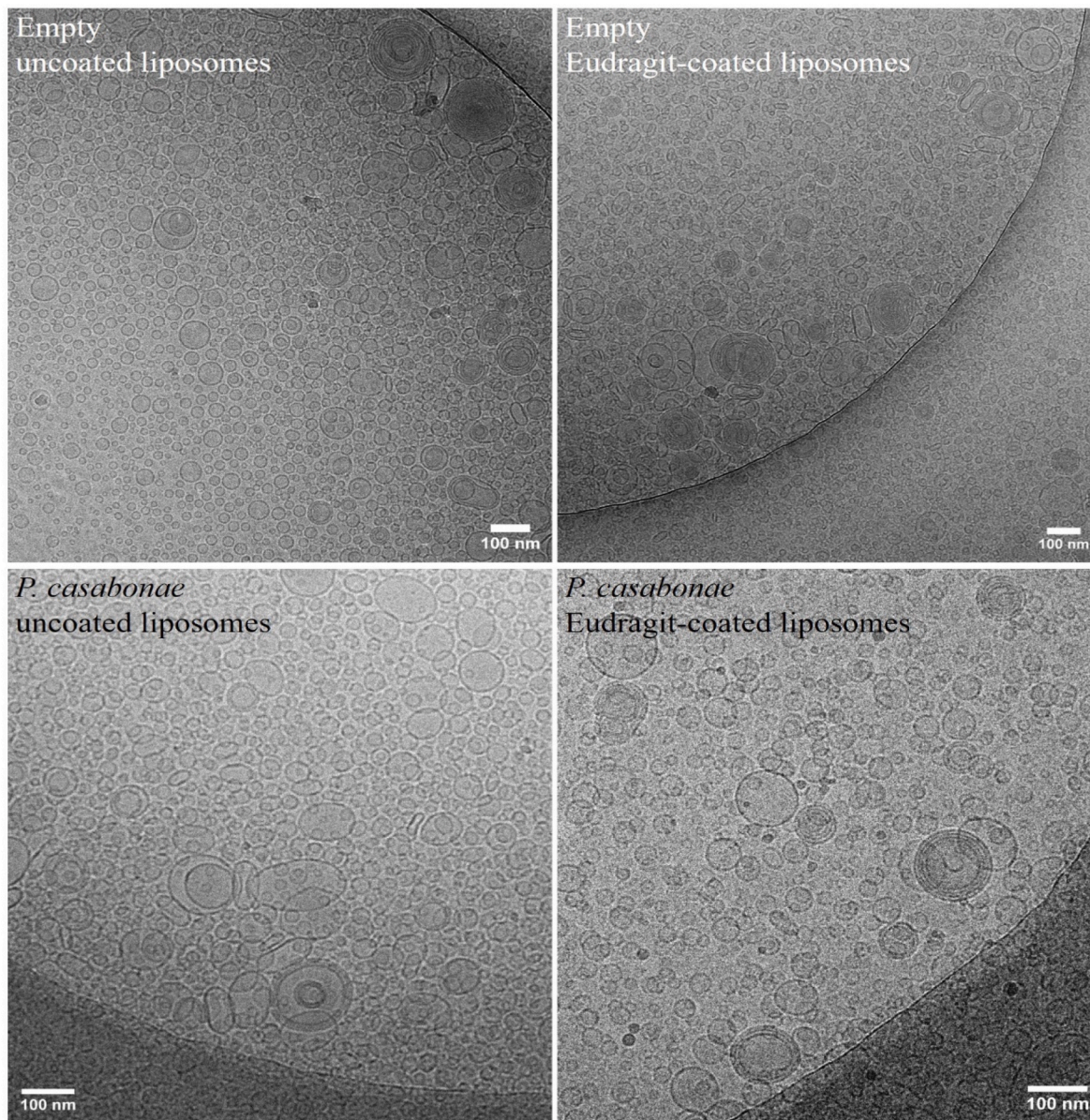


Fig. 2. Cryo-TEM micrographs of uncoated and Eudragit-coated liposomes, both empty and loaded with *P. casabonae* extract.

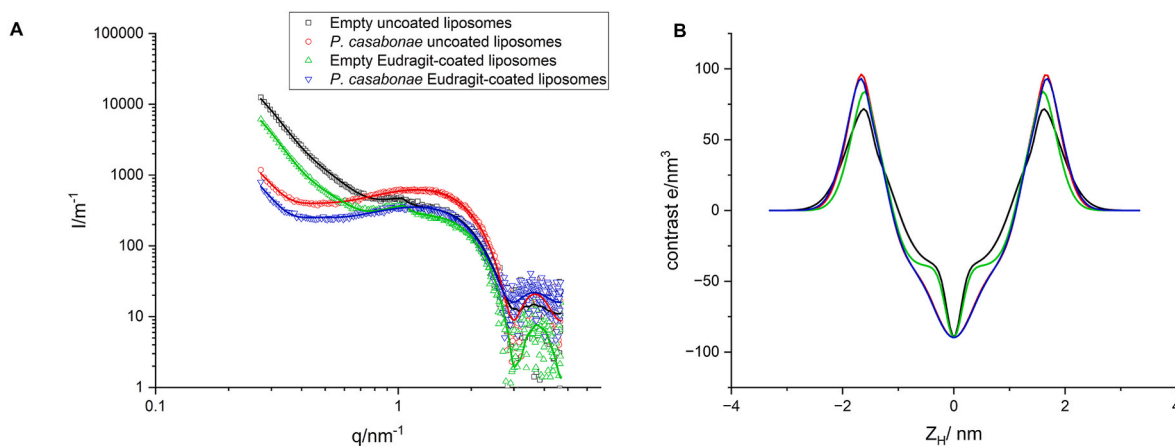


Fig. 3. A, SAXS patterns of uncoated and Eudragit-coated liposomes. The lines correspond to the fitted models and the symbols to the experimental points. Error bars are not shown for clarity, their magnitude is similar to the symbols up to 0.7 nm^{-1} , about twice the symbols up to 2.5 nm^{-1} and three times and larger from this point. B, Electronic density profiles of the bilayers corresponding to the fits in A.

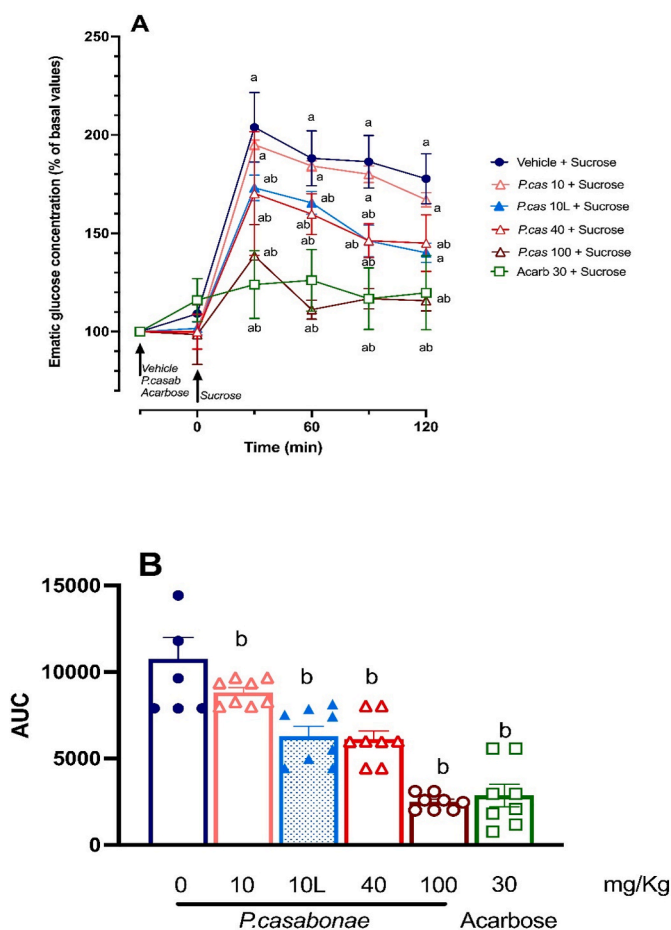


Fig. 4. Effect of intragastric administration of *P. casabonae* extract on blood glucose levels after sucrose challenge. Rats received an intragastric administration of 10, 40 or 100 mg/kg extract dissolved in vehicle (1 % Tween 80 in water), acarbose (30 mg/kg), or Eudragit-coated liposomes loaded with *P. casabonae* extract at a dose of 10 mg/kg (*P. casabonae* 10L). Data are mean \pm SEM ($n = 8$ rats per treatment) and are expressed as percent change from basal (time 0) glycemia (Panel A) and area under the curve (AUC; Panel B). ^a $p < 0.001$ vs. basal values; ^b $p < 0.001$ vs. control (vehicle-treated rats).

support of this hypothesis, we found no overt behavioral signs of toxicity in the animals after treatment with the extract, and none of them had died by the end of the experiments. In future research, this safety aspect will certainly be re-examined in relation to the active compounds that may be identified in the extract.

Considering our *P. casabonae* extract's chemical composition, we propose that the synergistic interaction of caffeoylquinic acid derivatives, flavonoids, and phenolic acids contributes to the observed antihyperglycemic effects. Notably, compounds such as caffeoylquinic acid derivatives (e.g. chlorogenic acid) and the flavonoids rutin and apigenin have been widely recognized for their positive impact on diabetes management by improving glycemic control, lipid profiles, and antioxidant defenses [25–28]. Both rutin and apigenin demonstrably lower blood glucose levels in animal models of diabetes [29–32], likely due to their potent antioxidant properties. Flavonoids play a crucial role in preventing the deterioration of pancreatic beta-cells and may facilitate the regeneration of damaged pancreatic cells [27]. Histopathological analyses of diabetic animals have shown that rutin can protect Langerhans islets from degeneration [33]. While most studies have explored the antihyperglycemic effects of flavonoids in diabetic animals (primarily using the streptozotocin-induced model of type 1 diabetes), Jadhav and Puchchakayala [34] reported rutin's blood glucose-lowering effects in both normal and diabetic rats, which aligns with our findings.

Table 4

Fitting parameters and derived parameters (\pm estimated error from the fit) for SAXS curve of *P. casabonae* Eudragit-coated liposomes vs. empty Eudragit-coated liposomes and uncoated liposomes. The parameters of the model are: χ^2 : reduced chi squared, d : repetition distance, η_1 : Caillé parameter, N_c : number of correlated bilayers; % of correlated bilayers, σ_H : polar head Gaussian amplitude, ρ_H : headgroup contrast electron density; Z_H : polar head Gaussian center, σ_C : methyl Gaussian amplitude. The additional spheres population parameters correspond to the polydispersity index PI of the Shultz distribution and the mean particle radius R .

SAXS parameters	Empty uncoated liposomes	<i>P. casabonae</i> uncoated liposomes	Empty Eudragit-coated liposomes	<i>P. casabonae</i> Eudragit-coated liposomes
χ^2	3.7	1.0	1.56	1.4
d (nm)	5.98 ± 0.08	–	5.93 ± 0.05	–
η_1	0.35 ± 0.01	–	0.31 ± 0.01	–
N_c	4.5 ± 0.1	1.0	3.5 ± 0.1	1.0
% correlated bilayers	26 ± 4	0	32 ± 3	0
σ_H (nm)	0.528 ± 0.006	0.316 ± 0.006	0.414 ± 0.006	0.328 ± 0.006
ρ_H (e/nm^3)	61 ± 1	106 ± 1	73 ± 1	102 ± 1
Z_H (nm)	1.42 ± 0.02	1.56 ± 0.02	1.47 ± 0.02	1.57 ± 0.02
σ_C (nm)	0.112 ± 0.005	0.337 ± 0.005	0.088 ± 0.005	0.346 ± 0.005
PI	0.24 ± 0.01	0.17 ± 0.01	0.22 ± 0.01	0.16 ± 0.01
R (nm)	11.25 ± 0.03	11.70 ± 0.03	11.04 ± 0.03	11.65 ± 0.03

Although flavonoids exhibit notable bioactivity in various *in vitro* systems, their biological effects *in vivo* are limited due to low bioavailability, which is primarily a result of poor solubility and limited membrane permeability [35]. Consequently, various strategies, including the development of delivery systems, have been suggested to enhance their bioavailability. In this study, to ensure and possibly enhance the delivery of *P. casabonae* extract, Eudragit-coated liposomes were proposed for its oral administration [36,37].

The intragastric injection of 10 mg/kg of *P. casabonae* extract formulated in Eudragit-coated liposomes produced a significant ($p < 0.001$) antihyperglycemic effect that was quantitatively similar to that obtained with the 40 mg/kg dose of the extract aqueous solution, as the glycemic peak was 73.1 ± 6.0 % and the AUC was reduced by 44 % (Fig. 4A and B). These results are clearly indicative of a significant improvement obtained by using the nanoformulated extract, as compared to an aqueous solution. Indeed, the vesicles enhanced the pharmacological action of the extract so that a 4-time lower dose was required to obtain the same antihyperglycemic effect as that of the 40 mg/kg dose of the aqueous solution. Similarly, Amato et al. [38] reported that the encapsulation in eudragit-containing liposomes allowed an extract from fermented grain to protect mouse retina from diabetic retinopathy-induced damage by preventing functional retinal failure, oxidative stress, inflammation, astrogliosis, cell apoptosis, vascular endothelial growth factor upregulation, and blood-retinal barrier breakdown at one-tenth of the concentration at which the free extract showed protective effects.

The specific pharmacokinetic mechanism that characterizes the favorable effect of *P. casabonae* Eudragit-coated liposomes was not addressed in the present study, but it is reasonable to assume that they increase the gastrointestinal absorption of the compounds present in the extract by increasing their bioavailability and facilitating diffusion across cell membranes. The formulation of *P. casabonae* extract in Eudragit-coated liposomes proved to be particularly effective, likely correlated with the high entrapment efficiency of the flavonoids rutin and apigenin, and may therefore be advantageous for the administration of lower doses of the extract (or their active compounds), thus reducing off-target actions and potential adverse effects.

However, it has to be noted that for the extract administered in its liposomal form, we were not able to test doses higher than 10 mg/kg, due to the concentration of the extract in the Eudragit-coated liposomes (2 mg/ml) and the limited volume that can be given intragastrically. Future investigation will be devoted to modifying the nanoformulation, in terms of qualitative-quantitative composition, to incorporate a higher amount of *P. casabonae* extract and increase the dose to be given to rats.

For the data shown in Fig. 4A, two-way ANOVA revealed a significant main effect of treatment [$F(5,42) = 4.411$; $P = 0.0001$]; a significant main effect of time [$F(2,585, 108.6) = 179.5$; $P < 0.0001$]; and a significant interaction between factors [$F(25,210) = 9.035$; $P < 0.0001$]. For the data reported in Fig. 4B, one-way ANOVA revealed that the treatment significantly affected AUC [$F(5,41) = 22.76$; $P < 0.0001$].

4. Conclusions

The present study highlights the antihyperglycemic effect of a hydroalcoholic extract from *P. casabonae* leaves. The extract decreased glucose levels in rats after a sucrose load in a dose-dependent manner, confirming the *in vitro* antidiabetic potential of the plant. Furthermore, the extract was successfully incorporated in a stable vesicular system, and its antihyperglycemic effect at low doses was enhanced by the nanoformulation. Overall, our findings suggest that *P. casabonae* could be a promising candidate to provide lead compounds for the management of diabetes, also in the form of a food supplement, since the plant is edible and traditionally consumed.

Further studies will be conducted to improve the loading capabilities of the liposomes, which in turn will increase the dose to be administered to rats intragastrically. Moreover, we also plan to test the extract in streptozotocin-lesioned rats to better characterize its antihyperglycemic effect in an experimental model of diabetes.

Funding

This publication was produced during Simone Pani's attendance of the PhD programme in Life, Environmental and Drug Sciences at the University of Cagliari, Cycle XXXVIII, with the support of a scholarship co-financed by the Ministerial Decree no. 352 of April 9, 2022, based on the NRRP – funded by the European Union – NextGenerationEU – Mission 4 "Education and Research", Component 2 "From Research to Business", Investment 3.3, and by the company Bioinnova S.r.l.s. (Potenza, Italy).

This research was partially funded by: Fondazione di Sardegna (2020, project ID: F75F21001280007); Spanish Government (AEI) and European Union (FEDER) under the project PID2021-12480B-I00; Generalitat de Catalunya under the project 2021 SGR 00507.

CRediT authorship contribution statement

Simone Pani: Writing – original draft, Investigation. **Carla Caddeo:** Writing – review & editing, Supervision, Investigation, Conceptualization. **Laura Dazzi:** Writing – original draft, Investigation. **Giuseppe Talani:** Investigation. **Enrico Sanna:** Writing – original draft, Investigation. **Arianna Marengo:** Writing – original draft, Investigation. **Patrizia Rubiolo:** Writing – review & editing, Validation. **Ramon Pons:** Writing – original draft, Investigation. **Aurélien Dupont:** Investigation. **Sonia Floris:** Investigation. **Cinzia Sanna:** Writing – review & editing, Writing – original draft, Investigation. **Francesca Pintus:** Validation, Funding acquisition, Conceptualization.

Declaration of competing interest

The authors declare that they have no known competing financial interests or personal relationships that could have appeared to influence the work reported in this paper.

Data availability

Data will be made available on request.

Acknowledgments

Jaume Caelles, from the SAXS-WAXS service at IQAC (Barcelona, Spain), is acknowledged for helping with SAXS determinations. The EDUC-Share project, funded by the European Union's Horizon 2020 research and innovation program under grant agreement No. 101017526, is gratefully acknowledged for financial support for the cryo-TEM measurements taken at the UNIVREN-BIOSIT-MRic core facility at the University of Rennes (France).

Appendix A. Supplementary data

Supplementary data to this article can be found online at <https://doi.org/10.1016/j.jddst.2024.106078>.

References

- [1] A. Negre-Salvayre, R. Salvayre, N. Augé, R. Pamplona, M. Portero-Otín, Hyperglycemia and glycation in diabetic complications, *Antioxidants Redox Signal.* 11 (2009) 3071–3109, <https://doi.org/10.1089/ars.2009.2484>.
- [2] R.F. Mapanga, M.F. Essop, Damaging effects of hyperglycemia on cardiovascular function: spotlight on glucose metabolic pathways, *Am. J. Physiol. Heart Circ. Physiol.* 310 (2015) H153–H173, <https://doi.org/10.1152/ajpheart.00206.2015>.
- [3] D. Aronson, Hyperglycemia and the pathobiology of diabetic complications, *Adv. Cardiol.* 45 (2008) 1–16, <https://doi.org/10.1159/000115118>.
- [4] D.J. Magliano, E.J. Boyko, I.D.F.D.A.t.e.s. committee, IDF diabetes atlas, in: *Idf Diabetes Atlas, International Diabetes Federation* © International Diabetes Federation, 2021. Brussels, 2021.
- [5] K. Papatheodorou, M. Banach, E. Bekiari, M. Rizzo, M. Edmonds, Complications of diabetes 2017, *J. Diabetes Res.* 2018 (2018) 3086167, <https://doi.org/10.1155/2018/3086167>.
- [6] Z. Tao, A. Shi, J. Zhao, Epidemiological perspectives of diabetes, *Cell Biochem. Biophys.* 73 (2015) 181–185, <https://doi.org/10.1007/s12013-015-0598-4>.
- [7] D.K. Patel, R. Kumar, D. Laloo, S. Hemalatha, Natural medicines from plant source used for therapy of diabetes mellitus: an overview of its pharmacological aspects, *Asian Pacific J. Tropic. Dis.* 2 (2012) 239–250, [https://doi.org/10.1016/S2222-1808\(12\)60054-1](https://doi.org/10.1016/S2222-1808(12)60054-1).
- [8] A.V. Patel, J. Rojas-Vera, C.G. Dacke, Therapeutic constituents and actions of *Rubus* species, *Curr. Med. Chem.* 11 (2004) 1501–1512, <https://doi.org/10.2174/0929867043365143>.
- [9] R. Verpoorte, Pharmacognosy in the new millennium: leadfinding and biotechnology, *J. Pharm. Pharmacol.* 52 (2000) 253–262, <https://doi.org/10.1211/0022357001773931>.
- [10] K.J. Willis, *State of the World's Plants 2017*, Kew: Royal Botanic Gardens, London (UK), 2017.
- [11] C. Sanna, A. Maxia, G. Fenu, M.C. Loi, So uncommon and so singular, but underexplored: an updated overview on ethnobotanical uses, biological properties and phytoconstituents of Sardinian endemic plants, *Plants* 9 (2020), <https://doi.org/10.3390/plants9080958>.
- [12] M. Fois, E. Farris, G. Calvia, G. Campus, G. Fenu, M. Porceddu, G. Bacchetta, The endemic vascular flora of sardinia: a dynamic checklist with an overview of biogeography and conservation status, *Plants* 11 (2022), <https://doi.org/10.3390/plants11050601>.
- [13] A. Marengo, A. Maxia, C. Sanna, M. Mandrone, C.M. Berteza, C. Bicchi, B. Sgorbini, C. Cagliari, P. Rubiolo, Intra-specific variation in the little-known mediterranean plant *Ptilostemon casabonae* (L.) Greuter analysed through phytochemical and biomolecular markers, *Phytochemistry* 161 (2019) 21–27, <https://doi.org/10.1016/j.phytochem.2019.02.005>.
- [14] C. Sanna, A. Fais, B. Era, G.L. Delogu, E. Sanna, L. Dazzi, A. Rosa, A. Marengo, P. Rubiolo, A. De Agostini, S. Floris, F. Pintus, Promising inhibition of diabetes-related enzymes and antioxidant properties of *Ptilostemon casabonae* leaves extract, *J. Enzym. Inhib. Med. Chem.* 38 (2023) 2274798, <https://doi.org/10.1080/14756366.2023.2274798>.
- [15] A.P. Rolo, C.M. Palmeira, Diabetes and mitochondrial function: role of hyperglycemia and oxidative stress, *Toxicol. Appl. Pharmacol.* 212 (2006) 167–178, <https://doi.org/10.1016/j.taap.2006.01.003>.
- [16] C. Caddeo, M. Gabriele, A. Nàcher, X. Fernández-Busquets, D. Valenti, A. Maria Fadda, L. Pucci, M. Manconi, Resveratrol and artemisinin eudragit-coated liposomes: a strategy to tackle intestinal tumors, *Int. J. Pharm.* 592 (2021) 120083, <https://doi.org/10.1016/j.ijpharm.2020.120083>.
- [17] M. De Luca, C.I.G. Tuberose, R. Pons, M.T. García, M.D.C. Morán, G. Ferino, A. Vassallo, G. Martelli, C. Caddeo, Phenolic fingerprint, bioactivity and nanoformulation of *Prunus Spinosa* L. fruit extract for skin delivery, *Pharmaceutics* 15 (2023), <https://doi.org/10.3390/pharmaceutics15041063>.
- [18] C. Caddeo, R. Pons, C. Carbone, X. Fernández-Busquets, M.C. Cardia, A. M. Maccioni, A.M. Fadda, M. Manconi, Physico-chemical characterization of

- succinyl chitosan-stabilized liposomes for the oral co-delivery of quercetin and resveratrol, *Carbohydr. Polym.* 157 (2017) 1853–1861, <https://doi.org/10.1016/j.carbpol.2016.11.072>.
- [19] A.E. Martin, P.A. Montgomery, Acarbose: an alpha-glucosidase inhibitor, *Am. J. Health Syst. Pharm.* 53 (1996) 2277–2290, <https://doi.org/10.1093/ajhp/53.19.2277>, quiz 2336–2277.
- [20] D. Wang, J. Liu, S. Qiu, J. Wang, G. Song, B. Chu, L. Li, G. Xiao, J. Gong, F. Zheng, Ultrasonic degradation kinetics and isomerization of 3- and 4-O-caffeoylquinic acid at various pH: the protective effects of ascorbic acid and epigallocatechin gallate on their stability, *Ultrason. Sonochem.* 80 (2021) 105812, <https://doi.org/10.1016/j.ultrsonch.2021.105812>.
- [21] D. Wang, J. Wang, J. Sun, S. Qiu, B. Chu, R. Fang, L. Li, J. Gong, F. Zheng, Degradation kinetics and isomerization of 5-O-caffeoylquinic acid under ultrasound: influence of epigallocatechin gallate and vitamin C, *Food Chem. X* 12 (2021) 100147, <https://doi.org/10.1016/j.fochx.2021.100147>.
- [22] D. Wang, Y. Wang, Z. Zhang, S. Qiu, Y. Yuan, G. Song, L. Li, T. Yuan, J. Gong, Degradation, isomerization and stabilization of three dicaffeoylquinic acids under ultrasonic treatment at different pH, *Ultrason. Sonochem.* 95 (2023) 106401, <https://doi.org/10.1016/j.ultrsonch.2023.106401>.
- [23] A. Catalán-Latorre, M. Pleguezuelos-Villa, I. Castangia, M.L. Manca, C. Caddeo, A. Nácher, O. Díez-Sales, J.E. Peris, R. Pons, E.J.N. Escribano-Ferrer, Nutriosomes: prebiotic delivery systems combining phospholipids, a soluble dextrin and curcumin to counteract intestinal oxidative stress and inflammation, *Nanoscale* 10 (2018) 1957–1969.
- [24] E. Etuk, Animal models for studying diabetes mellitus, *Agric. Biol. J. N. Am.* 1 (2010) 130–134.
- [25] F. Hajiaghaalipour, M. Khalilpourfarshbafi, A. Arya, Modulation of glucose transporter protein by dietary flavonoids in type 2 diabetes mellitus, *Int. J. Biol. Sci.* 11 (2015) 508–524, <https://doi.org/10.7150/ijbs.11241>.
- [26] A.K. Singh, H.K. Rana, V. Singh, T. Chand Yadav, P. Varadwaj, A.K. Pandey, Evaluation of antidiabetic activity of dietary phenolic compound chlorogenic acid in streptozotocin induced diabetic rats: molecular docking, molecular dynamics, in silico toxicity, in vitro and in vivo studies, *Comput. Biol. Med.* 134 (2021) 104462, <https://doi.org/10.1016/j.compbiomed.2021.104462>.
- [27] R. Vinayagam, B. Xu, Antidiabetic properties of dietary flavonoids: a cellular mechanism review, *Nutr. Metab.* 12 (2015) 60, <https://doi.org/10.1186/s12986-015-0057-7>.
- [28] C. Wu, X. Zhang, X. Zhang, H. Luan, G. Sun, X. Sun, X. Wang, P. Guo, X. Xu, The caffeoylquinic acid-rich *Pandanus tectorius* fruit extract increases insulin sensitivity and regulates hepatic glucose and lipid metabolism in diabetic db/db mice, *J. Nutr. Biochem.* 25 (2014) 412–419, <https://doi.org/10.1016/j.jnutbio.2013.12.002>.
- [29] A.A. Fernandes, E.L. Novelli, K. Okoshi, M.P. Okoshi, B.P. Di Muzio, J. F. Guimarães, A. Fernandes Junior, Influence of rutin treatment on biochemical alterations in experimental diabetes, *Biomed. Pharmacother.* 64 (2010) 214–219, <https://doi.org/10.1016/j.biopha.2009.08.007>.
- [30] N. Kamalakkannan, P.S. Prince, Antihyperglycaemic and antioxidant effect of rutin, a polyphenolic flavonoid, in streptozotocin-induced diabetic wistar rats, *Basic Clin. Pharmacol. Toxicol.* 98 (2006) 97–103, <https://doi.org/10.1111/j.1742-7843.2006.pto.241.x>.
- [31] H. Liu, P. Huang, X. Wang, Y. Ma, J. Tong, J. Li, H. Ding, Apigenin analogs as α -glucosidase inhibitors with antidiabetic activity, *Bioorg. Chem.* 143 (2023) 107059, <https://doi.org/10.1016/j.bioorg.2023.107059>.
- [32] S. Panda, A. Kar, Apigenin (4',5,7-trihydroxyflavone) regulates hyperglycaemia, thyroid dysfunction and lipid peroxidation in alloxan-induced diabetic mice, *J. Pharm. Pharmacol.* 59 (2007) 1543–1548, <https://doi.org/10.1211/jpp.59.11.0012>.
- [33] N.T. Niture, A.A. Ansari, S.R. Naik, Anti-hyperglycemic activity of rutin in streptozotocin-induced diabetic rats: an effect mediated through cytokines, antioxidants and lipid biomarkers, *Indian J. Exp. Biol.* 52 (2014) 720–727.
- [34] R. Jadhav, G. Puchchakayala, Hypoglycemic and antidiabetic activity of flavonoids: Boswellic acid, Ellagic acid, Quercetin, Rutin on streptozotocin-induced type 2 diabetic rats, *Int. J. Pharm. Pharmaceut. Sci.* 4 (2012) 251–256.
- [35] B. Gullón, T. Lú-Chau, M. Moreira, J. Lema, G. Eibes, Rutin: a review on extraction, identification and purification methods, biological activities and approaches to enhance its bioavailability, *Trends Food Sci. Technol.* 67 (2017), <https://doi.org/10.1016/j.tifs.2017.07.008>.
- [36] C. Caddeo, M. Gabriele, X. Fernández-Busquets, D. Valenti, A.M. Fadda, L. Pucci, M. Manconi, Antioxidant activity of quercetin in Eudragit-coated liposomes for intestinal delivery, *Int. J. Pharm.* 565 (2019) 64–69, <https://doi.org/10.1016/j.ijpharm.2019.05.007>.
- [37] D. Jain, A.K. Panda, D.K. Majumdar, Eudragit S100 entrapped insulin microspheres for oral delivery, *AAPS PharmSciTech* 6 (2005) E100–E107, <https://doi.org/10.1208/pt060116>.
- [38] R. Amato, A. Melecchi, L. Pucci, A. Canovai, S. Marracci, M. Cammalleri, M. Dal Monte, C. Caddeo, G. Casini, Liposome-mediated delivery improves the efficacy of Liosan G against retinopathy in diabetic mice, *Cells* 12 (2023), <https://doi.org/10.3390/cells12202448>.